Cell Tissue Res (1986) 243:273–288

Cell and Tissue Research

Neuroanatomy of the terminal (sixth abdominal) ganglion of the crayfish, *Procambarus clarkii* (Girard)

Yasuhiro Kondoh and Mituhiko Hisada
Zoological Institute, Faculty of Science, Hokkaido University, Sapporo, Japan

Summary. We studied the neuroanatomy of the terminal (sixth abdominal) ganglion in the crayfish *Procambarus clarkii* with silver-impregnated sections and nickel fills. We describe the fiber tracts, commissures and neuropilar areas, and give the topological relationships of motoneurons and intersegmental interneurons with reference to their neuropilar landmark structures.

All five anterior abdominal ganglia have an almost identical number of 600–700 neurons with a similar pattern of distribution. Each contains a single neuromere with a common plan of neuropil organization. In contrast, the terminal ganglion consists of two neuromeres which appear to be derived from the intrinsic sixth abdominal and 'telson' ganglion. The basic organization of each neuromere parallels that of the third abdominal ganglion in the appearance and arrangement of fiber tracts and commissures, although some modifications occur. The fusion of two neuromeres is represented by the duplication of segmentally homologous neurons, MoGs and LGs, whose topological relationships to the neuropil structures are similar to those of the anterior ganglion.

We also discuss the origin of the telson and its ganglion (the seventh abdominal neuromere), and dispute the classical theory that the telson derives from a 'postsegmental region.'

Key words: Abdominal ganglion – Neuroanatomy – Nickel-filling – Silver impregnation – *Procambarus clarkii*

For students of invertebrate neuroethology, the terminal (sixth abdominal) ganglion of the crayfish has been one of the most attractive subjects among invertebrate central nervous systems; many of its local and projecting interneurons have been well characterized physiologically and morphologically, and their role in sensory integration and the generation of motor output has been extensively studied (Takahata et al. 1981; Sigvardt et al. 1982; Reichert et al. 1982, 1983; Hisada et al. 1984; Nagayama et al. 1983). Because of the duplication of their serially homologous neurons, it has been suggested that the terminal ganglia of the crayfish and lobster consist of at least two fused embryonic ganglia (Johnson 1924). As long ago as 1928, Monton, in studying embryogenesis in decapods, noted that the terminal ganglion is derived from two fused embryonic ganglia. Nevertheless, there have been no systematic investigations on neuroanatomy of the terminal ganglion. Many basic questions, such as the number of fused ganglia and the extent to which the neuropil organization is modified in the course of fusion as well as the organization of the ganglion itself, remain to be answered. This situation is in striking contrast to the case of some insects, particularly with regard to the body ganglia of locusts and the brain of flies, for which detailed anatomical maps of the ganglia have been effectively drawn (Gregory 1974; Tyrer and Gregory 1982; Strausfeld 1976).

Until now, none of ganglionic structures of crustacean CNS have been characterized except for the brain (Helm 1928; Maynard 1966; Sandeman and Luff 1973), although the gross anatomy of the third abdominal ganglion of crayfish and the fourth abdominal ganglion of the hermit crab have been studied using silver-impregnated materials (Kendig 1967; Chapple and Hearney 1976). Recent studies by Skinner (1979, 1985) have described the architecture of the fourth abdominal ganglion of *Procambarus clarkii* and have produced a neuronal map. In the present account, we summarize initially the neuropil organization of the third abdominal ganglion with reference to that of the fourth abdominal ganglion (Skinner 1979, 1985) to show the basic framework of the crayfish abdominal ganglia. We then relate in detail the neuropil architecture of the terminal ganglion to that of the third abdominal ganglion. We emphasize in particular the duplex arrangement of neuromeres in the terminal ganglion; each of them is basically organized according to a common plan exhibited by the anterior abdominal ganglion, a plan that provides anatomical evidence for the origin of the terminal ganglion. We then proceed to describe the topological organization of motoneurons and intersegmental interneurons to show the functional organization of the ganglion. We shall deal separately with intraganglionic sensory projections of the afferent pathway.

Materials and methods

Animals. Crayfish, *Procambarus clarkii* Girard, of 10–12 cm in body length were used in this study.

Counting of cells. The number and distribution of the neurons were elucidated by examining whole-mount preparations and serial sections of ganglia stained with toluidine

Send offprint requests to: Yasuhiro Kondoh, Zoological Institute, Faculty of Science, Hokkaido University, Sapporo 060, Japan

blue (Altman and Bell 1976). Freshly dissected ganglia were stained in a borax-buffered (pH 7.6–9.0) toluidine blue solution (1%) for 20 min at 50° C. The ganglia were then fixed and destained with a formol-acetic acid-alcohol fixative (Strausfeld 1976) until an appropriate differentiation was obtained. For sectioning, ganglia were conventionally embedded in paraffin (Merck) and cut horizontally at a thickness of 20 μm. Whole-mount preparations were cleared in methyl benzoate and mounted in Biorite (Oken Shoji Co.).

The number of neurons were estimated from drawings made with a camera lucida drawing tube. Cells having the following features were counted as neurons: (1) large spherical nuclei (in contrast to glia cells with small elliptical nuclei), and (2) cytoplasm heavily stained by toluidine blue. Erroneous double counting of cells with large nuclei, which appeared in several serial sections, was avoided by repeated examination of the drawings.

Silver impregnation. The ganglia to be stained were fixed immediately after excision in alcoholic Bouin's fixative (Gray 1954) for 2 h at room temperature. They were stained with eosin in 90% alcohol (Pantin 1948) during dehydration to allow them to be oriented for sectioning, and then embedded in paraffin with melting points of 53°–55° C. Sections were cut to a thickness of 20 μm along the transverse, horizontal and sagittal planes, and impregnated by the Holmes-Blest method (Blest and Davie 1980).

Axonal fillings with nickel chloride. The projections of peripheral nerves were examined by axonal fillings with nickel chloride and subsequent silver intensification (Pitman et al. 1972; Bacon and Altman 1977; Sandeman and Okajima 1973). Each ganglion and its nerve trunks were dissected out in van Harreveld's crayfish saline. The cut ends of peripheral nerves or connectives were exposed to a 150–300 mM nickel chloride solution for 4–8 h at the room temperature or at 4° C. The tissues were then developed for 1 h in saline solution containing 4 or 5 drops per 10 ml of a saturated solution of rubeanic acid in alcohol (Quicke and Brace 1979; Delcomyn 1981), and then fixed in a formol-acetic acid-alcohol fixative. Silver intensification was done routinely on whole-mount specimens. Some of these were dehydrated in a series of alcohols, cleared and mounted in Biorite. Others were then refixed for 1 h in 1% osmium tetroxide in distilled water, washed, dehydrated in acetone and then embedded in epoxy resin (Quetol 812, Nisshin EM Co.). Serial sections 20 μm thick were cut.

The number and size of the motor axons in the relevant peripheral nerves of the terminal ganglion were determined by examining 3-μm thick Epon sections. Whole ganglia and their nerves were dissected out and fixed with alcoholic Bouin's fixative. Immediately after the fixation the tissues were dehydrated in acetone and embedded in epoxy resin. Sections were cut and stained with toluidine blue.

Abbreviations. The names of the fiber tracts used in this paper are based upon those used by Kendig (1967) and Skinner (1985), although some of them have been newly devised. The nomenclature of peripheral nerve trunks is that of Larimer and Kennedy (1969). The tracts and other structures will be generally referred to by their abbrevations, as listed below. If it is necessary to discriminate the individual ganglion, the abdominal ganglion number proceeds the description of the components. For example, the 'lateral giant interneuron of the third abdominal ganglion' is abbreviated as A3LG. *A1–5* first to fifth abdominal ganglia; *A6* sixth abdominal segment of the terminal ganglion; *A7* seventh abdominal segment of the terminal ganglion; *AVC* anterior ventral commissure; *CNS* central nervous system; *DCI-IV* dorsal commissures I–IV; *DIT* dorsal intermediate tract; *DLT* dorsal lateral tract; *DMT* dorsal medial tract; *DT* dorsal tract; *DV1–11* dorso-ventral tracts 1–11; *eLG* extra (posterior) lateral giant interneuron; *LDT* lateral dorsal tract; *LG* lateral giant interneuron; *LVT* lateral ventral tract; *MDT* median dorsal tract; *MG* medial giant interneuron; *MoG* motor giant neuron; *Np* neuropil; *MVT* median ventral tract; *PVC* posterior ventral commissure; *R1–7* nerve roots 1–7; *R1m–3m* motor fiber tracts of nerve roots 1–3; *R1s–3s* sensory fiber tracts of nerve roots 1–3; *SCI-II* sensory commissures I–II; *VIT* ventral intermediate tract; *VLT* ventral lateral tract; *VMT* ventral medial tract; *VMTi-ii* ventral median tracts i-ii.

Results

The number and distribution of neurons in the abdominal ganglion

We found that the number of neurons per abdominal ganglion was within the range of 600–700 (Table 1), with no significant difference between the sexes. Although, in general, neurons could be readily identified, difficulties were encountered in the anterolateral margin of the five anterior ganglia and in the ventro-medial cell layer of the terminal ganglion. These areas contained small nerve cell bodies with

Table 1. The number of neurons in crayfish abdominal ganglia

References	Specimen	The number of neurons in the abdominal ganglia (not including those neurons in the nerve roots)					
		1st	2nd	3rd	4th	5th	6th
Wiersma (1957)	I	527	445	517	532	498	520
	II	–	628	–	–	649	–
Roth and Supper (1973)	adult	–	–	770	–	–	670
	3rd to 4th instar	–	–	550	–	–	480
Reichert et al. (1982)		–	–	–	–	–	630–651
Present study	I	687	641	656	638	612	638
	II	664	655	–	634	592	678

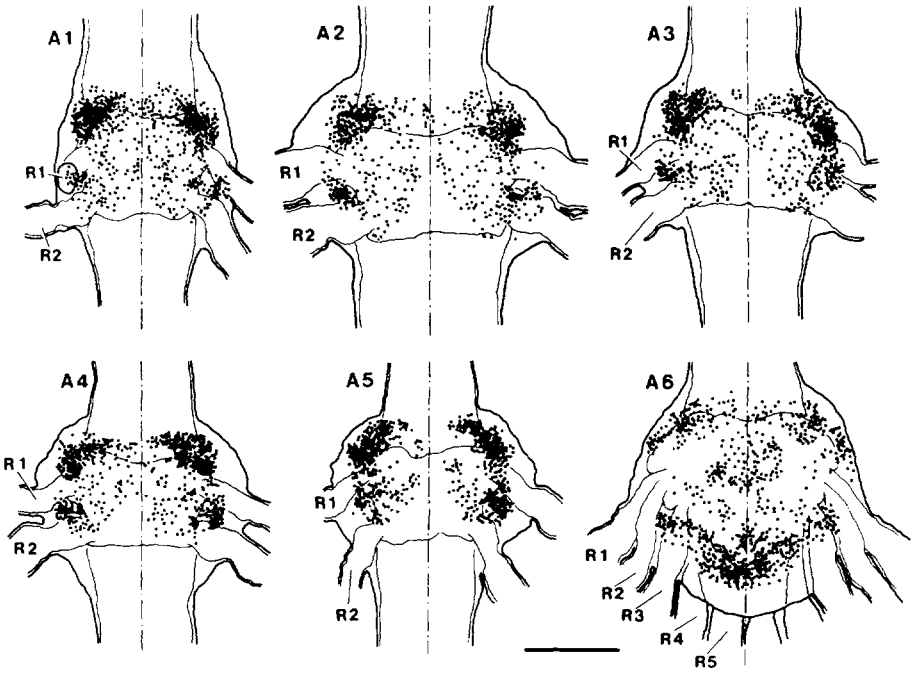

Fig. 1. Distribution of neurons in all abdominal ganglia on the horizontal plane. The centers of neuronal cell bodies are plotted. Thin lines demarcate the borders between glial cell layer and neuropil. Nerve R6 and R7 are not drawn in the terminal ganglion. The anterior part is at the top. Scale: 300 μm

little cytoplasm; this made it difficult to distinguish them from glial cells, and, especially in the terminal ganglion, to count.

Reconstructions from serial sections (Fig. 1) demonstrated that the anterior five ganglia have much the same pattern of distribution of nerve cell bodies. On the other hand, the terminal ganglion was found to differ in the following respects: a group of small cells (20–30 μm in diameter) lies near the midline of the ventral cortex of the ganglion, while a second group of about 70 cells (30–40 μm) associated with nerve R7 is found at the posterior end of the ganglion.

General structure of the ganglion

The Holmes-Blest impregnation method used in this study selectively stains the sheath, perineurium, nuclei but not cytoplasm of glial cells, neuropil, neural fibers and cell bodies of the neurons (Fig. 2). The ganglia are enclosed within a sheath and perineurium under which lies a thick layer of large glial cells (cortical glial cells, Abott 1970, 1971). These glial cells also lie between neural cell bodies and the neuropil, occupying an extensive region of the ganglion. Moreover, a number of elliptical nuclei of glial cells were observed to lie around the neuronal cell bodies and in the neuropil, particularly near the midline. On the dorsal surface of the ganglion and connectives, there are two pairs of giant axons, medial giant (MG) and lateral giant (LG).

The five anterior ganglia consisting of single neuromeres are clearly organized according to a common plan. We therefore provide here a brief description of the organization of the third abdominal ganglion (A3) as a representative of all of them. (For a more detailed description of the fourth abdominal ganglion, see Skinner, 1985). Figure 3 illustrates transverse and horizontal sections showing the principal features of the neuropil in A3, where all of the major structures in the fourth abdominal ganglion can be found. The ten longitudinal tracts, which run between the anterior and posterior connectives, are the most prominent (Fig. 3): from dorsal to ventral, DT, DLT, DIT, DMT, VLT, VIT, VMT, LVT, and MVT. The DT, which runs dorsally over the dorsal commissures, DCI-IV, consists of two sub-tracts, MDT and LDT. DLT, VIT, and VLT run separately from each other in the anterior half of the ganglion core (Fig. 3A), although they are collected into a single tract that runs under the axonal bundles of nerve R2 (Fig. 3C). VMT separates dorsoventrally into two well-defined bundles (VMTi and VMTii). VMTi runs over the horseshoe neuropil (HN), whereas the VMTii lies under it (Figs. 3C, 3F, 5A). In the posterior connectives, the motor axons of nerve R3, which originate between DCIII and DCIV, run posteriorly dorsal to MDT (Fig. 3D).

Nine prominent transverse tracts (commissures), which interconnect the two hemispheres of the ganglion, can be readily distinguished in sagittal section near the midline (Fig. 5A): DCI-IV, VCI-III, AVC and HN. The most dorsal, DCI-IV, lies across the midline of the ganglion between MDT and DMT, which contain many thick neurites of motoneurons running though nerve R2 and R3. The VCIII contains a pair of primary neurites of the LGs which cross the midline at the anterior region of VCIII, slightly posterior to the MoG. Under VMT lie the most ventral commissures, AVC (Figs. 3A, E), which cross the midline at the anterior edge of the neuropil. HN, which is a region of fine fibered neuropil, lies between VMTi and VMTii (Fig. 3C). A small posterior commissure, PVC, lies between the right and left VMT.

Repetitive arrangement of commissures in the terminal ganglion

Reconstruction from silver-impregnated sections (Fig. 2) clearly demonstrated that the terminal ganglion consists of two fused neuromeres, the sixth (A6) and seventh (A7) abdominal neuromeres. These two neuromeres fuse completely with each other (Fig. 2E) so that the limit between them

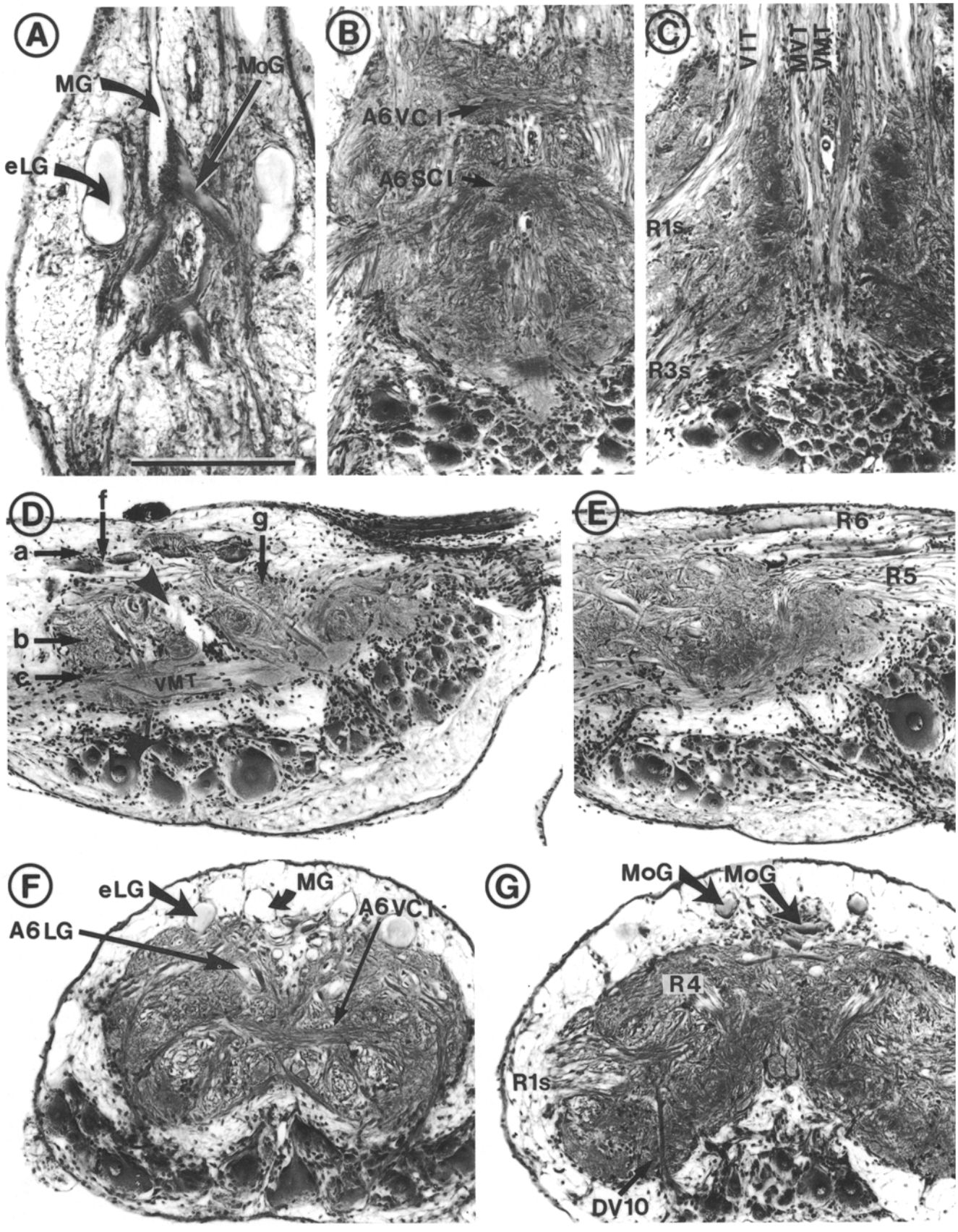

Fig. 2A–G. Microphotographs of silver-impregnated sections of the terminal ganglion on the horizontal (**A, B, C**), sagittal (**D, E**) and transverse (**F, G**) planes, orientations given in 1**D** (*arrows* a, b, c, f and g). The *arrowhead* in **D** indicates the midline cleft of the ganglion. The anterior part is at the top in the horizontal sections and at the left in the sagittal sections. The dorsal part is at the top in the transverse sections. Scale: 300 μm

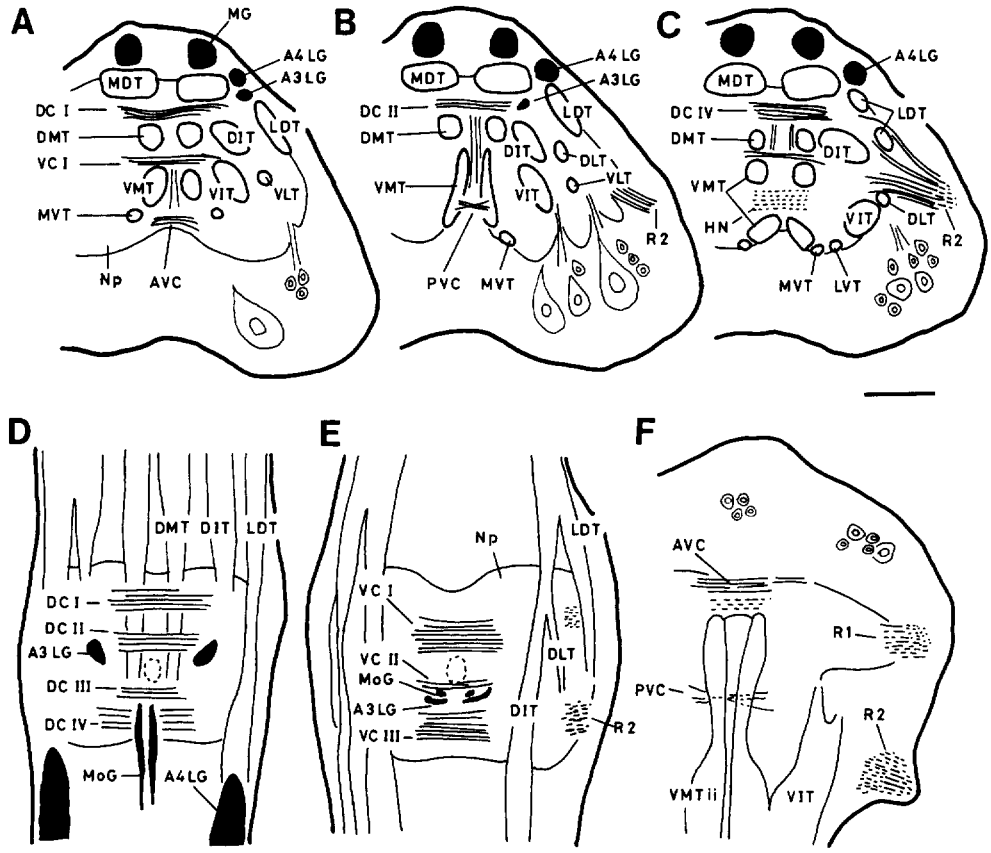

Fig. 3A–F. Drawings of sections of the third abdominal ganglion, showing the major structures of the neuropil. Broken line circles (center, in **D, E**) indicate the central canal of the ganglion, which contains numerous glial cells. Scale: 300 μm.
A–C Transverse sections arranged from the anterior to the posterior parts. The dorsal part is at the top.
D–F Horizontal sections are arranged from the dorsal to the ventral side. The anterior part is at the top

can be discriminated only by the midline cleft (Fig. 2D arrowhead) into which numerous glial cells insert themselves. The basic organization of the core in each neuromere is similar to that in A3 (Fig. 5A), though there are slight modifications. There are two dorsal (A6DCI-II) commissures, three intermediate (A6VCI-III) ones and a single ventral (A6AVC) commissure in the intrinsic A6 neuromere (Fig. 5B). The A6SCI, which lie across the ganglion midline under the VCIII, is a region of finely fibered neuropil in addition to HN in A3; it is designated here as a *sensory commissure* because of its special association with the projection of primary afferents. No conspicuous tracts comparable to PVC in A3 were found under VMT. The arrangement of commissures in A7 neuromere is modified rather extensively (Fig. 5B). There is one dorsal commissure, A7DCI, above DMT, three intermediate commissures, A7VCI-III, between DMT and VMT, and two ventral commissures, A7AVC and A7PVC, under VMT. Sensory commissures, A7SCI-II, also form a region of finely fibered neuropil into which the primary afferents of nerves R3, R4 and R5 project (Kondoh and Hisada, in preparation). The A7SCI located posterior to A7VCI-II is a unique structure found only in the A7 neuromere.

The ganglionic fusion of two neuromeres is represented also by the duplication of segmentally homologous neurons. The most typical of these are the lateral giant interneurons (LGs) and the motor giant neurons (MoGs) whose topological relationships to the fiber tracts and commisures are parallel to those of A3 (Fig. 4). Two pairs of LGs, the ordinary sixth abdominal segment and an extra LG segment (Johnson 1924; Kondoh and Hisada 1983), lie in the dorsal part of the terminal ganglion (Fig. 2A, F). Cell bodies lie side by side in the posterior end of the ganglion contralateral to their thick neurites. The primary neurites transverse the midline of the posterior intermediate commissures, A6VCIII and A7VCIII, which lie under the DMT (Fig. 4B), as is found in LG of A3 (Fig. 4D).

Topological similarities among MoGs in A3, A6, and A7 neuromeres are also obvious (Fig. 4A–D). The MoG neurite in A3 invades the neuropil between DCIII and DCIV obliquely and then runs ventrally just anterior to the primary neurites of LGs (Fig. 4D, C). Two pairs of MoGs in the terminal ganglion share the structural features of their anterior homologous (Mittenthal and Wine 1978; Selverston and Remler 1972) (Figs. 2A, 4E): large cell bodies with a diameter of 100–120 μm, simple dendritic contacts with a terminal of a medial giant interneuron (MG) and thick axons (60–80 μm in diameter). Their primary neurites run near the midline just anterior to the primary neurites of A6LGs and of eLGs (Fig. 4A, B).

Longitudinal and vertical fiber tracts

The system of longitudinal tracts in the A6 neuromere is largely similar in appearance and arrangement to that in A3: within the core of the ganglion, ten longitudinal tracts can be readily distinguished (Fig. 7A–C). The dorsal tracts MDT, LDT, DLT, DIT and DMT terminate to ramify in the posterior half of the ganglion. In contrast, ventral tracts including VMT, VIT, VLT, MVT and LVT run through the ganglion core to enter the peripheral nerves. Of these, VMT consists largely of the axonal bundles of

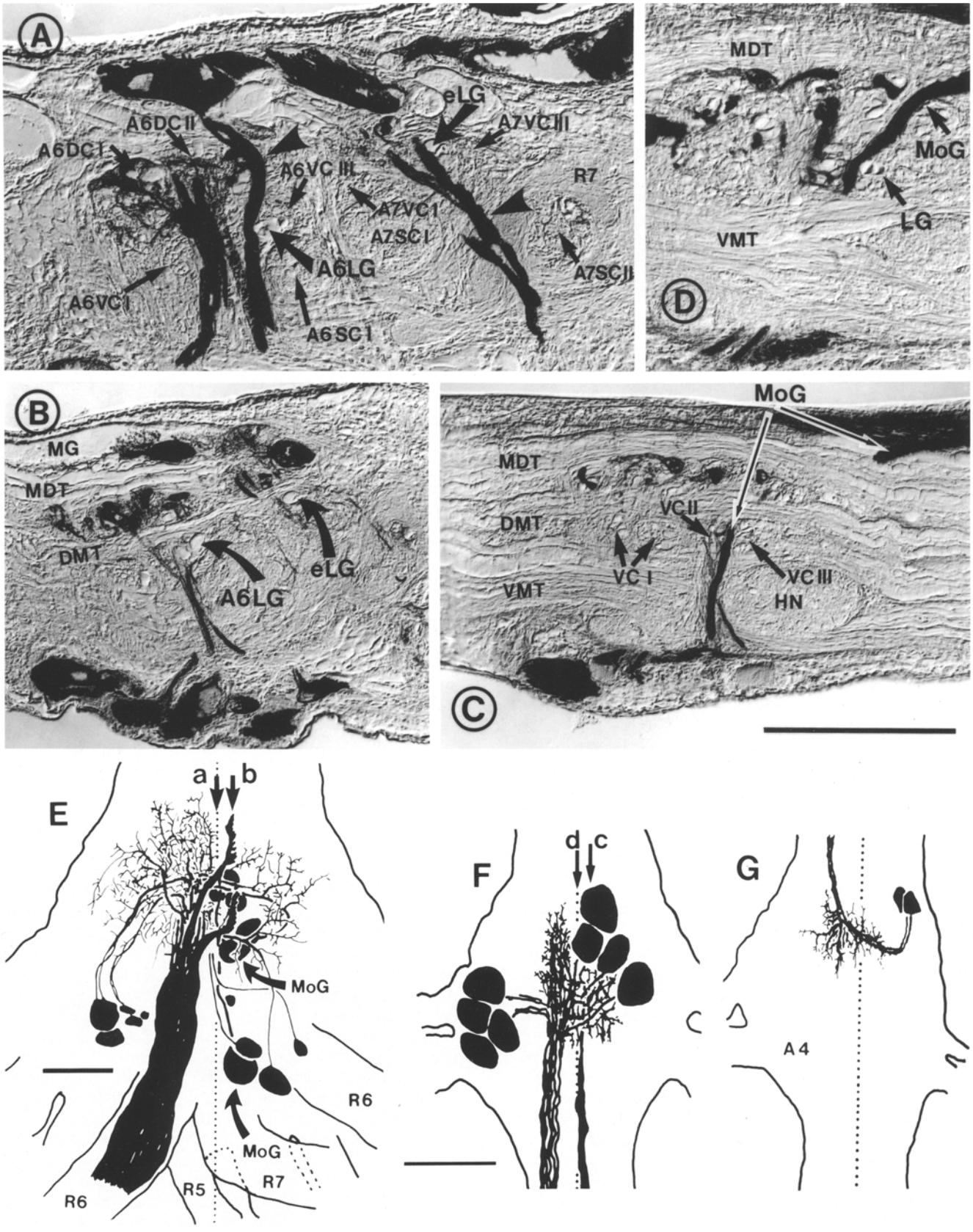

Fig. 4A–G. The topological organization of MoGs and the other fast flexor motoneurons, revealed by nickel fills and subsequent silver intensification. Scale (for **A–D** shown in **C** and **F, G** in **F**): **B, C, F, G** 300 μm; **A, D, E** 200 μm. **A, B** Sagittal sections near the midline of the terminal ganglion. Note that the anterior and posterior MoGs (*arrowheads*) run dorsoventrally just anterior to the A6LG and eLG (*arrows*), respectively, orientations given in **E** (*arrows* a and b). **C, D** Sagittal sections of the third abdominal ganglion, orientations given in **F** (*arrows* c and d). **E** Camera lucida drawing (ventral view) of telson flexor motoneurons, showing the central branching pattern, dendritic fields and locations of cell bodies. **F, G** Camera lucida drawings of the fast flexor motoneurons in the third abdominal segment, viewed ventrally; of these, eight neurons lie in the third abdominal ganglion and two cells lie in the fourth abdominal ganglion. The anterior part is at the top

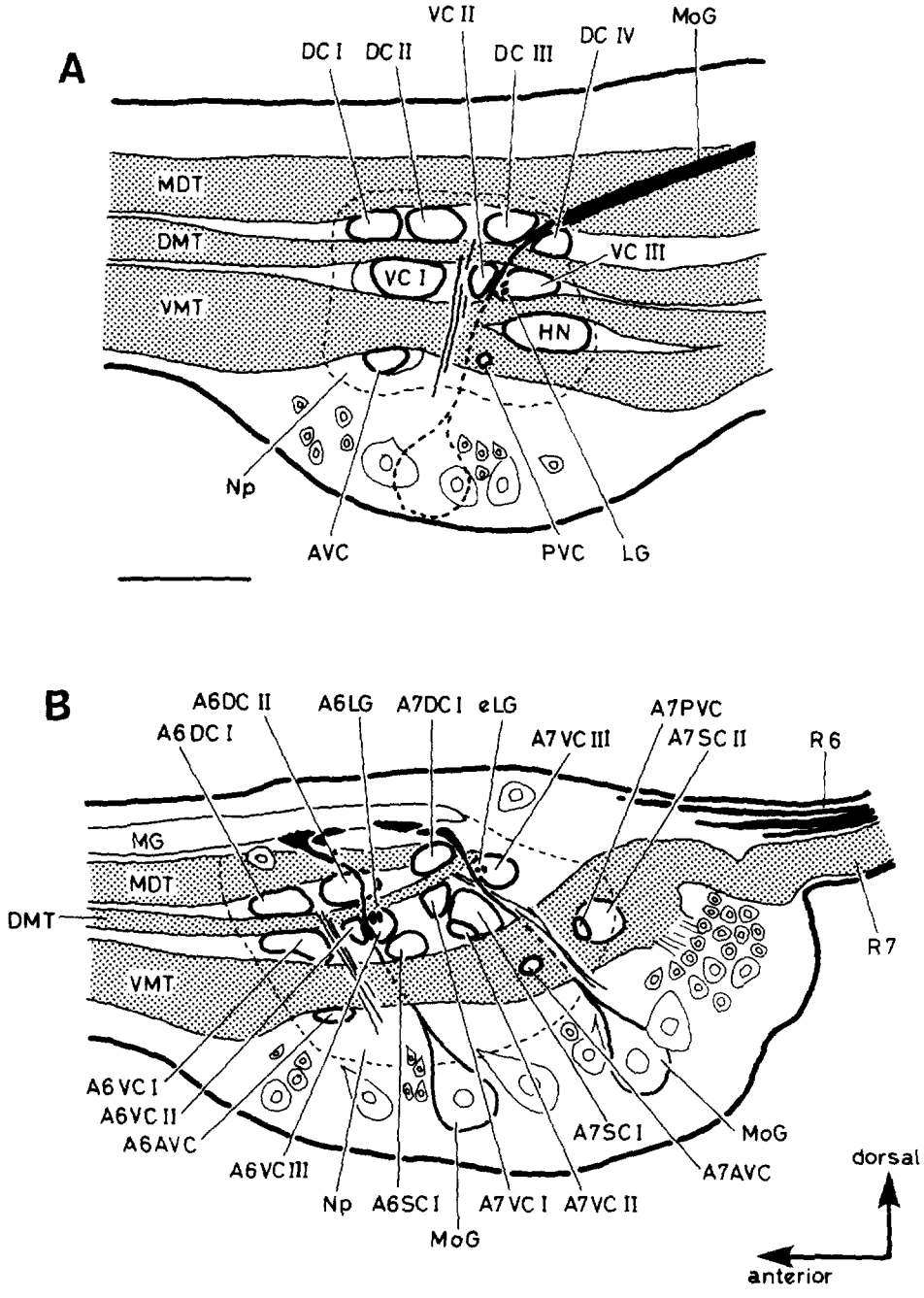

Fig. 5A, B. Schematic drawings of the sagittal section of the third abdominal (**A**) and terminal (**B**) ganglion at the midline, showing the arrangement of commissures, longitudinal fiber tracts (*hatched*) and the central pathways of MoGs and LGs. Scale: 300 μm

neurons associated with nerve R7, which innervates the hind gut (Winlow and Laverack 1972) (Figs. 12, 13); the rest are exclusively associated with the sensory projection of five paired nerves.

Primary neurites of neuronal cell bodies are grouped into several fiber bundles for insertion into the neuropil. Some tracts are distinct and may form useful landmarks. They are designated as *dorsoventral tracts* (DV), and are numbered according to their position from the anterior to posterior parts (Fig. 8). DV1 and DV2 (I-tracts of Kendig 1967) lie between A6VCI and A6AVC to interconnect them dorsoventrally. The primary neurites of the telson flexor motoneurons form three prominent tracts, DV3, DV4 (J and M-tracts of Kendig 1967, respectively) and DV6. In the anterolateral region of the neuropil two vertical tracts, DV7 and DV8, lie between the DIT and DLT (Fig. 8D–F). DV9 and DV10, which are prominent in transverse sections (Fig. 7E, F), run in the posterolateral region of the neuropil. DV11 runs obliquely between fiber bundles of peripheral axons from nerve R2 and R3. It consists of primary neurites of motoneurons associated with nerve R3 and of many local interneurons (Fig. 11A). In the midline cleft between A6VCIII and A7SCI several thick fibers associated with nerve R7 run obliquely to form DV5 (Figs. 8A, 13D).

Details of the neuropil

The basic anatomical features of the terminal ganglion are illustrated in Figs. 6 and 7. We give here a detailed descrip-

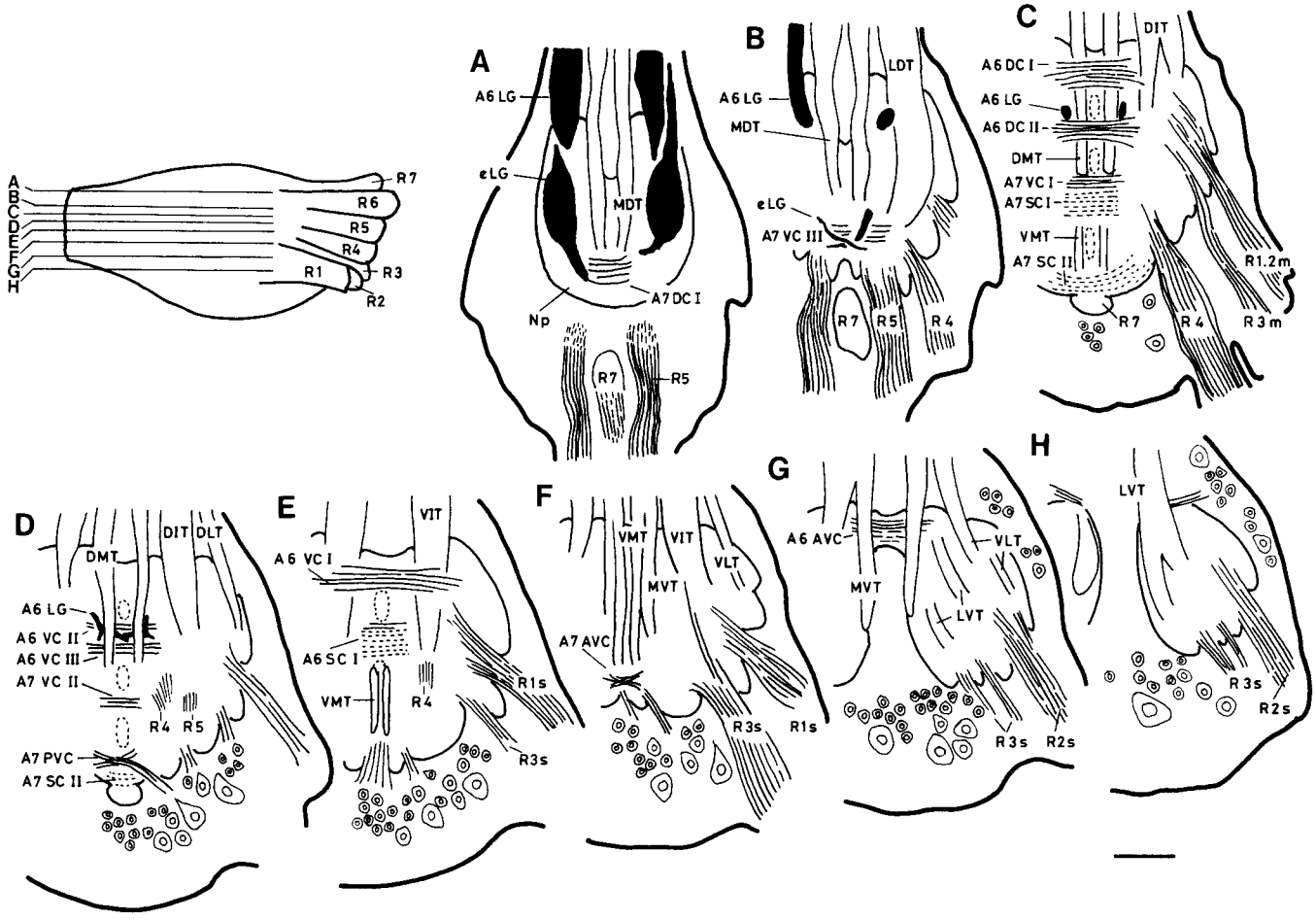

Fig. 6A–H. Reconstructed horizontal sections of the terminal ganglion in planes **A–H** are shown in lateral view of the ganglion at the left. Broken line circles indicate the midline cleft and canals formed by glial cells. Scale: 200 μm

tion based mainly on horizontal sections and supplementarily upon transverse sections.

The dorsal region of the neuropil at the dorsal commissure level (Fig. 6A–C). Axons of MG, eLG and flexor motoneurons (MoG and nerve R6) lie on the dorsal surface of the neuropil (Fig. 2A). Two commissures, A6DCI-II, lie in the anterior half of the ganglion between MDT and DMT, which run near the midline slightly medially to A6LG (Fig. 7A, B). They consist of relatively thick neurites composed largely of motoneurons (Fig. 4A, B). MDT and LDT run over the dorsal commissures, A6DCI-II, to terminate by fusing with A7DCI and A7VCIII (Fig. 9C). Of these, the latter runs posteriorly under the LG and eLG. In the A7VCIII, a pair of neurites of eLG crosses the midline (Fig. 6B).

The medial region of the neuropil at the level of intermediate commissures (Fig. 6C–E). Under DMT, there are three transverse tracts (A6VCI-III) and one sensory commissure (A6SCI) in the anterior half of the ganglion. The posterior commissures, A6VCII and III, are separated by the primary neurites of MoG, under which lies A6SCI. Primary sensory axons of nerve R1 entering from the ventrolateral edge of the neuropil run anteriorly mainly via the VIT. A pair of large neurites of an identified local sensory interneurons, LDS (Reichert et al. 1982, 1983), cross the midline in the A6DCII, providing an useful landmark. In neuromere A7 lie three transverse fiber tracts, A7DCI-III and two sensory commissures, SCI-II (Fig. 7E, F). Near the midline, A7AVC, A7PVC and A7SCII are enclosed by the axons associated with nerve R7 (Fig. 13C, D). The neurites of the motoneurons in nerves R1, R2, and R3 occupy the dorsolateral region of the neuropil into which DLT and DIT insert themselves before diffusion.

Ventral region of the neuropil (Fig. 6F–H). Near the midline run two longitudinal tracts, VMT and MVT, under which the primary neurites from the anterior cluster of neuronal cell bodies cross the midline to make up A6AVC (Fig. 9D). The small commissure, A7AVC, lies at the posterior end of the neuropil, in which the main neurites from some caudal cells of ascending interneurons cross the midline (Figs. 7G, 9E). Sensory fiber bundles of nerves R2 and R3 (R2s and R3s) enter the ventral region of the neuropil beneath the projection of nerve R1s. On the ventral surface of the neuropil lie two longitudinal tracts, LVT and MVT (Fig. 7A–G). LVT, VIT, and VLT are major tracts for the ascending projection of the primary afferents.

Tracts of ascending interneurons

The ventral commissures can be well characterized by the contents of the primary neurites of their ascending inter-

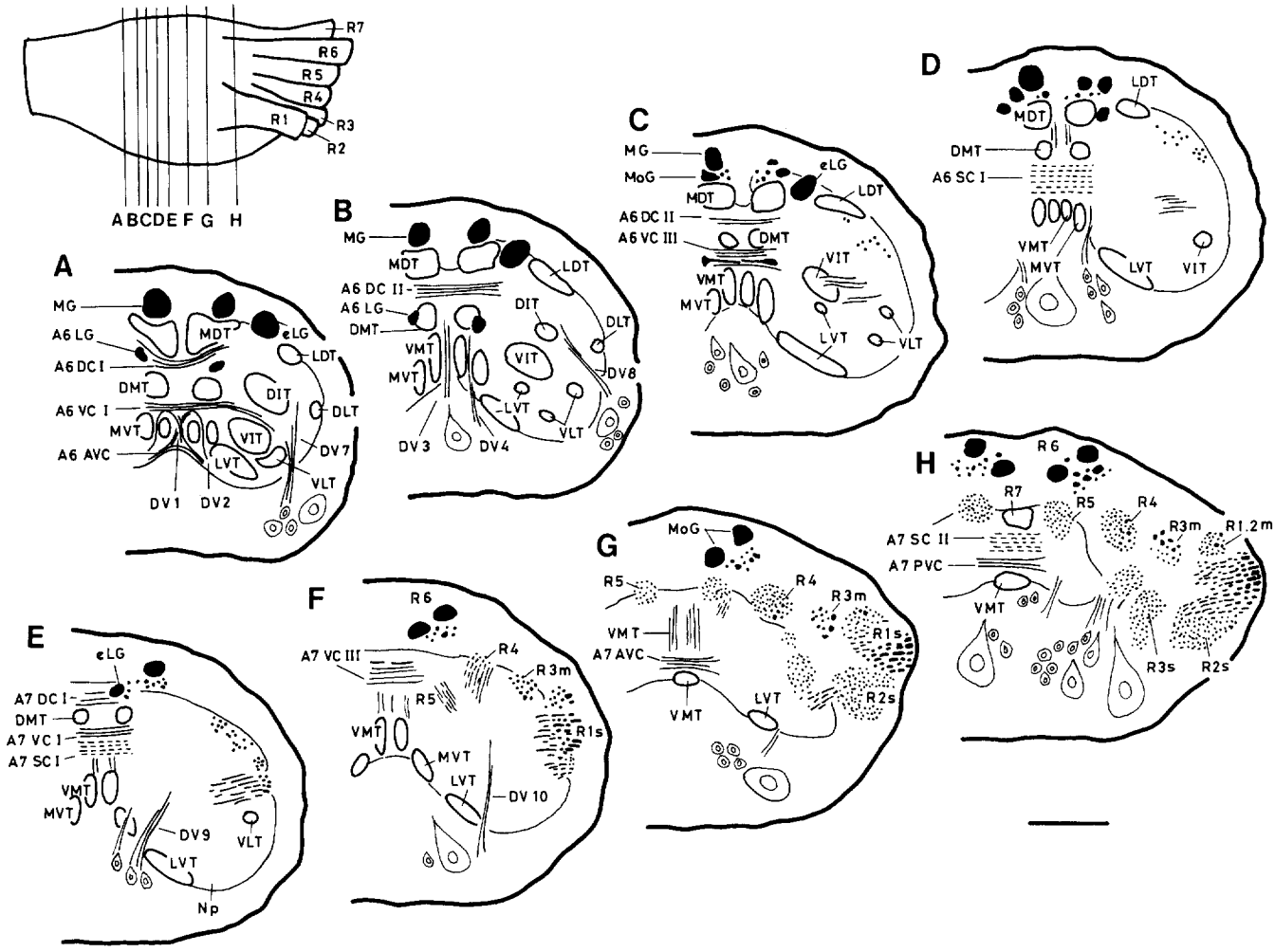

Fig. 7A–H. Transverse sections of the terminal ganglion in planes **A–H** shown in lateral view of the ganglion at the left. Scale: 200 μm

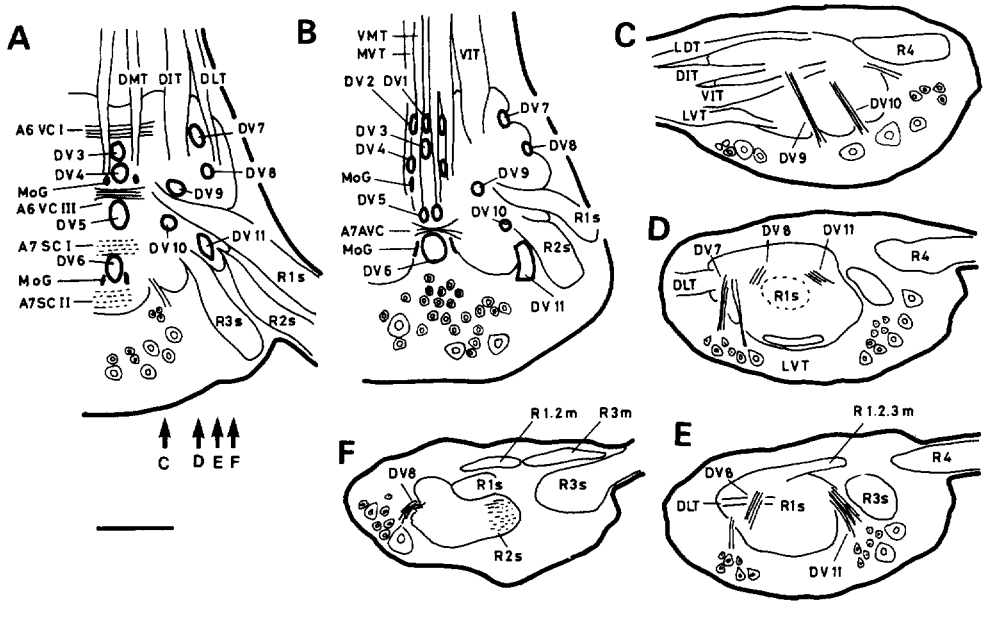

Fig. 8A–F. Arrangement of the dorsoventral tracts in the terminal ganglion. Scale: 300 μm.
A, B Horizontal sections. The anterior part is at the top.
C–F Sagittal sections, orientations given in **A**. The anterior is at the left

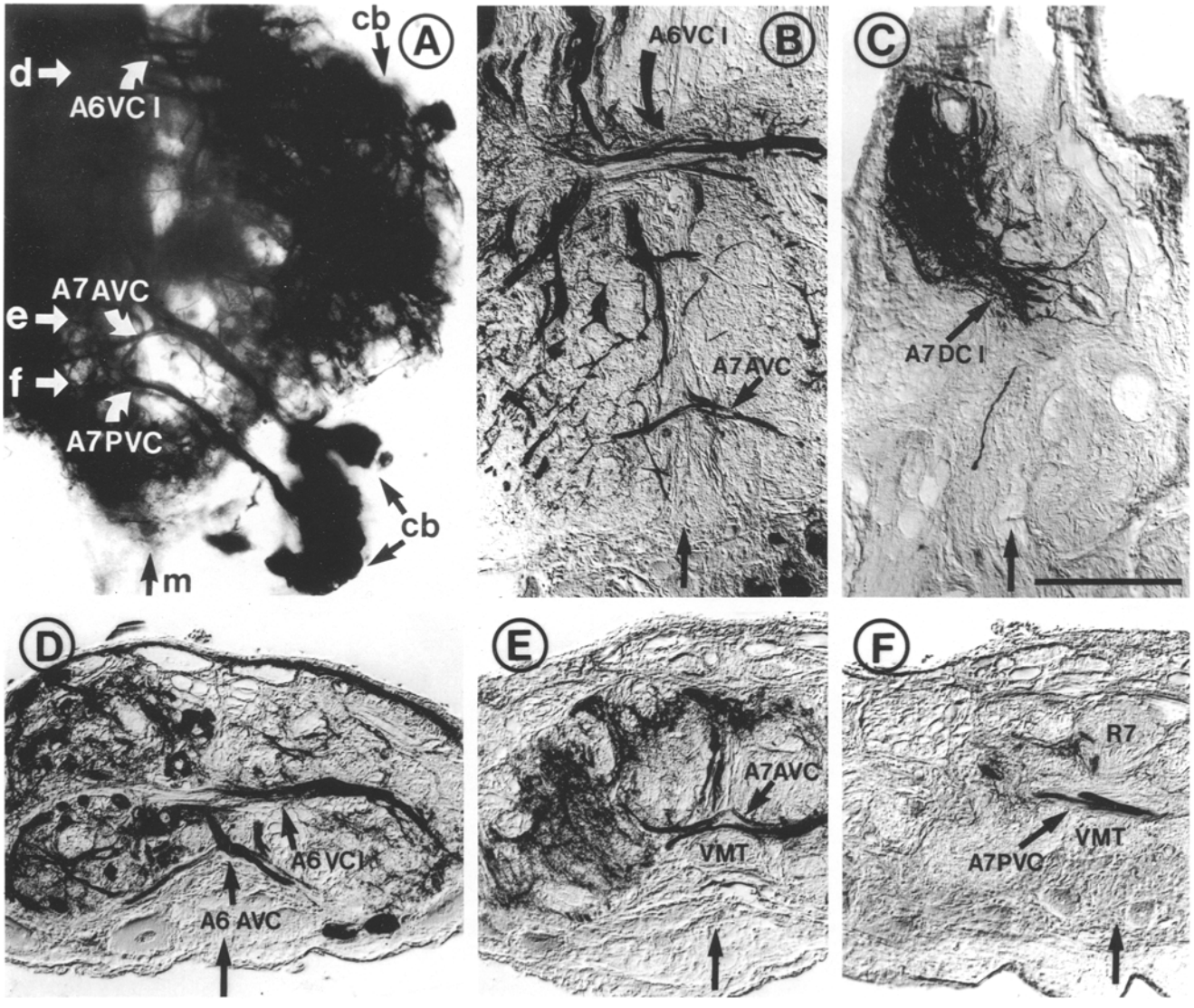

Fig. 9A–F. Microphotographs of a whole-mount (**A**) and sectioned (**B–F**) terminal ganglion stained by axonal fillings with nickel chloride via the cut end of anterior hemiconnective and silver intensification. Scale: 200 μm. In **A, B, C** the anterior part is at the top and in **D, E, F** the dorsal part is at the top. **A** A whole-mount preparation filled via anterior right commissure in the terminal ganglion, viewed ventrally. Note that almost all the contralateral cell bodies of the ascending interneurons lie across the midline in A6VCI, A6AVC, A7AVC and A7PVC. *Arrowheads* d, e, and f indicate the planes of section D, E, F, respectively; *cb* cell bodies of ascending interneurons, *m* midline. **B** A horizontal section at the plane of A6VCI and A7AVC through which the primary neurites of the ascending interneurons cross the midline. **C** A horizontal section at the plane beneath the MG, showing that descending fibers in the MDT and LDT turn medially to cross the midline at the A7DCI. **D–F** Transverse sections at the level of A6VCI and A6AVC (**D**), A7AVC (**E**) and A7PVC (**F**) as major fiber tracts of the ascending interneurons

neurons; these were revealed clearly by nickel fills via the cut end of the A5–A6 connective. Fig. 9 shows the location of their cell bodies and the topological organization of the primary neurites in relation to commissures and fiber tracts. In total, 86 cell bodies associated with the ascending interneurons were stained in each half of the ganglion. Most of them lie in the cortex contralaterally to the ascending axons (Fig. 9A), but a few cells are ipsilateral. The primary neurites originating from those cell bodies, which lie in the anterolateral region of the ganglion, cross the midline in A6AVC and A6VCI (Fig. 9B, D); they ascend largely via the VIT. However, some of them run medially along the anteroventral edge of the neuropil (Fig. 9D) and turn dorsally to project A6VCI via DV1 and DV2 before crossing the midline (Fig. 9D). In contrast, the posterolateral cells extend primary neurites toward the midline, which then run into A7AVC (Fig. 9B, E) and A7PVC (Fig. 9F) to cross the midline; they ascend via the LVT and MVT.

Motoneuronal geometry

There are six pairs of nerves (R1–6) and one unpaired nerve (R7) originating from the terminal ganglion. Their innervations have previously been reported (Larimer and Kennedy 1969; Sandeman 1982). The number and size of axons in the relevant motor branches of the peripheral nerves are shown in Table 2, and the number, size and position of cell bodies of motoneurons in Table 3. With regard to

Table 2. The number and size of the axons of motoneurons in the peripheral nerves of the terminal ganglion

Nerves	Number of axons	Diameter (No. of axons)
R1	8	20–30 μm (7); 10 μm (1)
R2	24	30–40 μm (4); 10–20 μm (17); <10 μm (3)
R3	31	50–60 μm (3); 30–40 μm (2); 20–30 μm (3); 10–20 μm (16); <10 μm (7)
R6	16	50–80 μm (2); 20–30 μm (8); <20 μm (6)

Table 3. Number, size and position of cell bodies of motoneurons in the terminal ganglion (best estimates)

Nerve	Total number of cells	Position (No.)	Size (No.)
R1	8	anterior ventral (7)	40–50 μm
		midline (1)[a]	40–50 μm
R2	23	anterior ipsilateral (16)	60–70 μm (2); 40–50 μm (1); 30–40 μm (8); 20–30 μm (2); 10–20 μm (3)
		ventrolateral (4)	10–20 μm
		caudal (2)	10–20 μm
		midline (1)[a]	40–50 μm
R3	27	near the midline (5)	60–80 μm (3); 20–30 μm (2)
		ventrolateral (3)	50–70 μm (2); 20–30 μm (1)
		caudal (19)	60–80 μm (3); 30–50 μm (7); 20–30 μm (9)
R4	1	ipsilateral (1)	20–30 μm
R5	1	anterior contralateral (1)	20–30 μm
R6	16	anterior contralateral (7)	60–100 μm (4); 20–30 μm (3)
		posterior contralateral (4)	60–100 μm (3); 20–30 μm (1)
		posterior ipsilateral (5)	50–60 μm (1); 20–30 μm (4)
R7	71	near the midline	
		dorsal (1–3)	30–50 μm
		anterior ventral (2–3)	30–50 μm
		caudal (65)	20–40 μm

[a] An identical neuron

nerves R2 and R3, we failed to stain the same number of cell bodies of motoneurons as expected from the thin sections of the nerves. We do not yet known whether this was the result of missing some cell bodies by the nickel filling method or because of counting as double or triple the branched axons that originate from a single neuron.

There are eight motoneurons associated with the first branch of the nerve R1 innervating muscles (Fig. 10A). One of these, the midline cell, sends its bifurcated axons to nerve R2 in addition to R1 (Fig. 10A, arrow). Primary neurites originating from cell bodies in anteroventral edge of the ganglion run dorsally to the dorsal neuropil via DV7, where they turn posteriorly and then run together with those of the motoneurons in nerve R2 within the dorsal neuropil (Fig. 11A).

Motoneurons innervating nerve R2 and R3 are strikingly similar in the location of their cell bodies, neurites, dendritic fields and axons. Twenty-three cell bodies associated with nerve R2 and 28 cell bodies with nerve R3 were found in the anterolateral, medial and posterolateral regions of the cortex of the ganglion (Table 3, Fig. 10B, C). The primary neurites originating from lateral and posterior cells run dorsally via DV7, DV8 and DV11. They turn abruptly posteriorly in the dorsal neuromere where they lie horizontally parallel to each other; the axons of nerve R2 are located laterally to those of nerve R3. Their major dendritic fields are restricted to the dorsomedial neuropil over the VIT, although they send lateral branches to the ventrolateral region of the neuropil (Fig. 11B–E). Posteriorly, some branches extending posteromedially reach the midline to project the A7SCII.

Sixteen cell bodies were stained in our best fills, as might be expected from the thin sections of nerve R6 (Fig. 4E). Their central branchings are confined entirely to the dorsomedial region of the neuropil (Fig. 4A, B). All transverse branches and neurites were confined to the A6DCI-II and A7DCI, whereas those of MoG transverse above the MDT.

Nerve R7, an unpaired median nerve innervating the hind gut, contains about 70 neurons. Most of these neurons lie in the caudal medial and of the ganglion but a few cells occur in the ventromedial and dorsomedial regions of the ganglion (Fig. 12, Table 2). Additionally, nickel fills via nerve R7 revealed one medial cell near the midline of the fifth abdominal ganglion (Fig. 12C). The axons and dendrites run near the midline to form the VMT (Fig. 13A, D) in which three commissures, A7AVC, A7PVC and A7SCII (Fig. 13B, C), cross the midline. Some thick fibers from R7 run dorsoventrally along the boundaries of the commissures (Fig. 13D).

Discussion

At the end of the last century, Retzius (1892) and Allen (1894), who studied the CNS of decapods in detail using Golgi impregnation and methylene blue staining, presented the earliest description of the cellular neuroanatomy of an arthropod CNS. In our own day, the recent advent of intracellular staining techniques (Pitman et al. 1972; Stretton and Kravitz 1968; Stewart 1978) has revitalized our interest in the cellular anatomy of the crustacean CNS. In these studies, the morphology of intracellularly stained cell were given in detail to include the fine dendritic branches, but their positions were plotted roughly inside the contour of the ganglion. Their relation to other neurons or intraganglionic structures was always difficult to assess because of the lack of any overall anatomical study of crustacean CNS apart from the brain (Helm 1928; Maynard 1966; Sandeman and Luff 1973). Our present findings should remedy this lack of information, all the structures characterized should provide useful landmarks as a guide through this particular region of the neuropil.

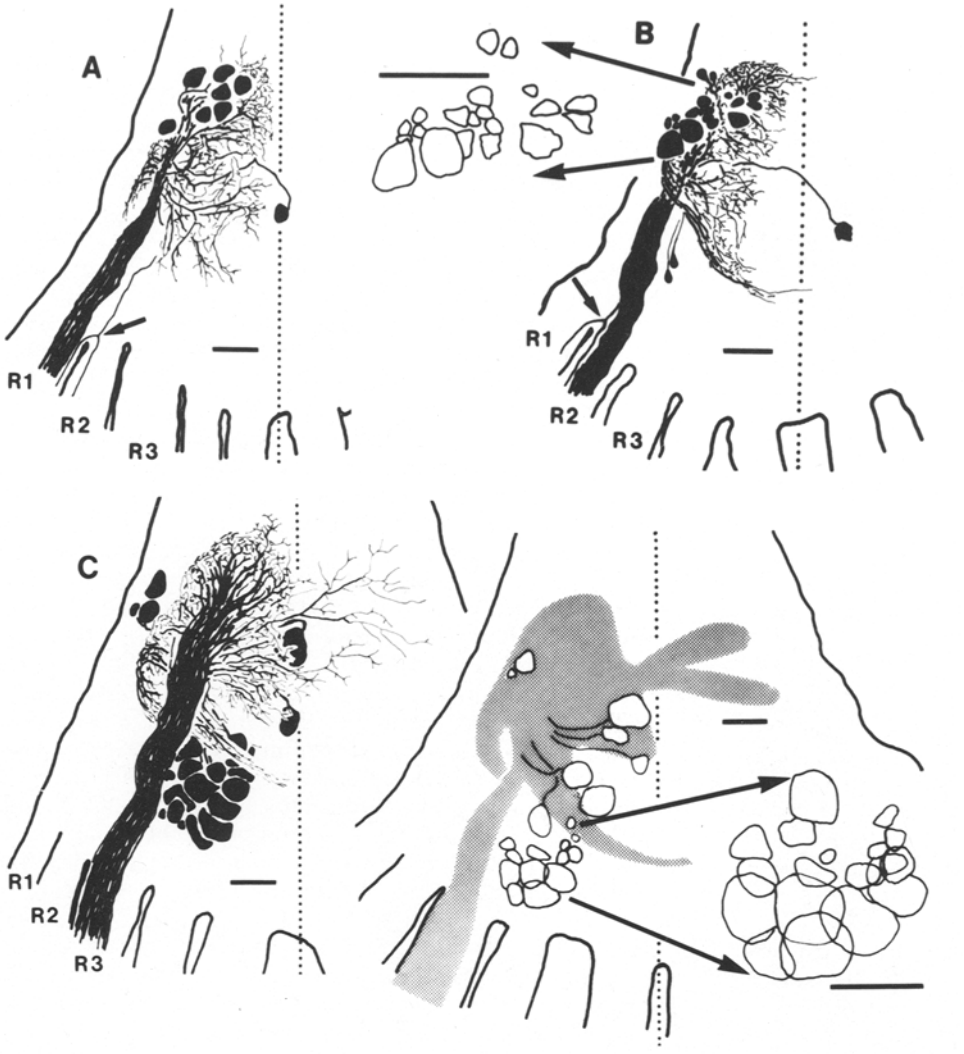

Fig. 10 A–C. Whole-mount drawings of $NiCl_2$-filled motoneurons in nerves R1 (**A**), R2 (**B**) and R3 (**C**) in the terminal ganglion, showing the location of cell bodies and central branching patterns, viewed ventrally (**A, B**) and dorsally (**C**). Scale: 100 μm

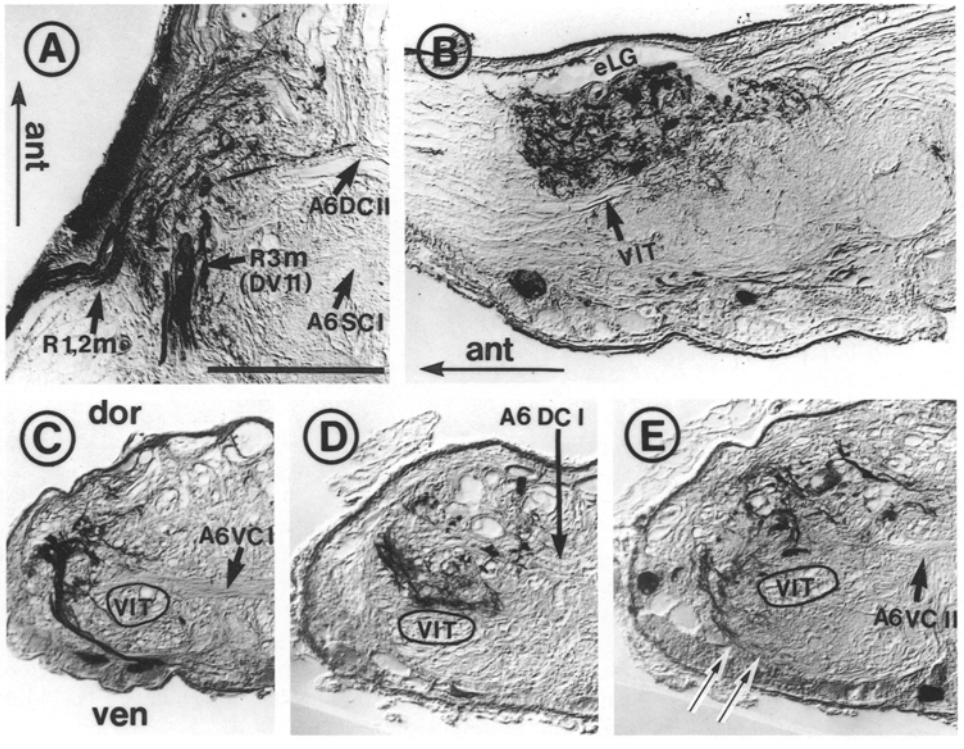

Fig. 11 A–E. Nomarski optic microphotographs of sections of $NiCl_2$-filled motoneurons in nerves R1, R2 and R3, showing their topological organization; *dor* dorsal, *ven* ventral, *ant* anterior. Scale: 300 μm.
A A horizontal section at the level of the A6DCII from the preparation in which R1m, R2m and R3m were filled simultaneously.
B A sagittal section near the midline, showing the dendritic fields of motoneurons in nerves R2 and R3; those are restricted to the antero-dorsal neuropil over the VIT to beneath the neurites of eLGs.
C A transverse section of R2 motoneurons.
D, E Transverse sections of R3 motoneurons in the posterior neuromere; they extend their lateral branches (unmarked *arrows*) to the ventral neuromere where sensory fibers in nerves R2 and R3 project extensively

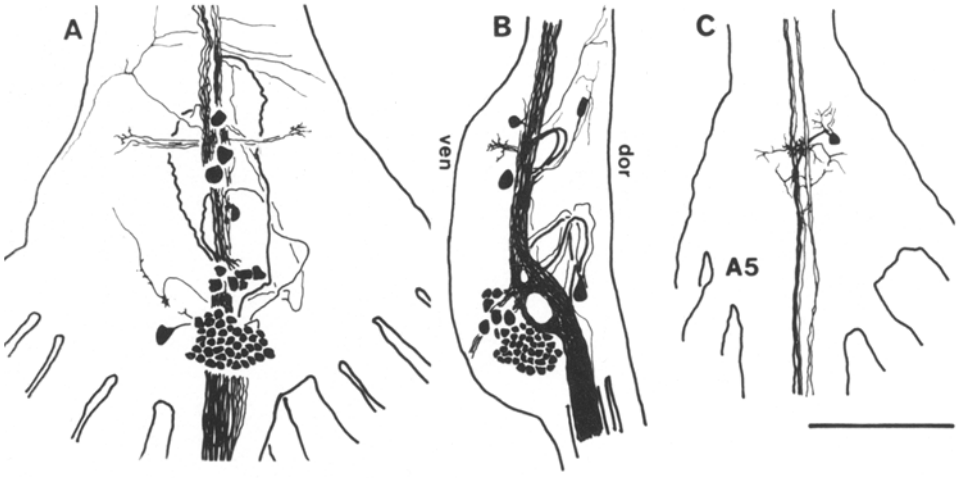

Fig. 12A–C. Camera lucida drawings of whole-mount preparations backfilled from the cut end of nerve R7. The anterior part is at the top. Scale: 500 μm.
A A ventral view of the terminal ganglion.
B A lateral view; *dor* dorsal, *ven* ventral.
C A ventral view of the fifth abdominal ganglion

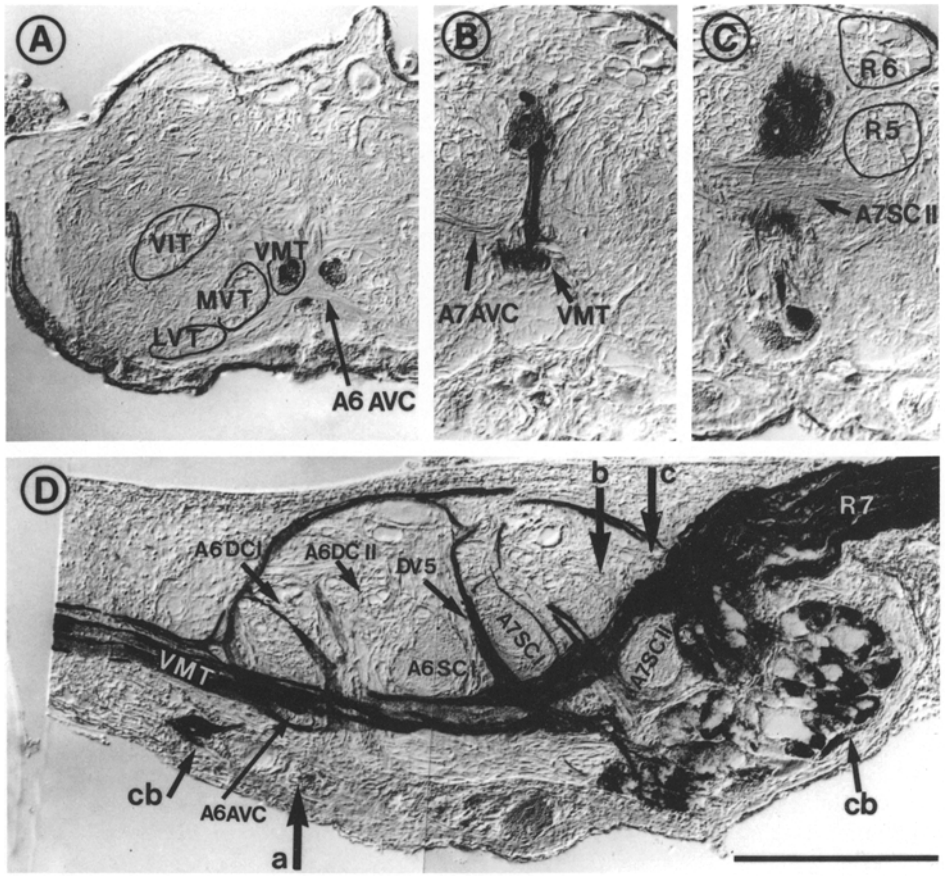

Fig. 13A–D. Nomarski optic microphotographs of ganglia stained by axonal fillings of nerve R7, showing the relationships of it central projection. Scale: 300 μm.
A–C transverse sections, orientations given in **D** (*vertical arrows* a, b and c). The dorsal part is at the top.
D A sagittal section near the midline. The VMT are stained selectively. Several fibers run horizontally through the dorsal region of the neuropil and dorsoventrally between the commissures; *cb* cell bodies associated with nerve R7

The segmentally common and specific distribution of neurons

The total number of neurons in each segmental ganglia of the crayfish abdomen has been counted by several workers (Table 1). Some appear to underestimate and some to overestimate. Either of these faults would be the result from a failure to follow up cells with small diameter and little cytoplasmic volume, which are difficult to distingush from glial cells and from each other. Our counts show, however, that all the abdominal ganglia have almost an identical number of neurons within a range of 600–700. Using computer-aided techniques, Macagno (1980) counted the precise neuronal number in the leech central nervous system and found segment specific differences: sex ganglia have a large number of additional cells. Our counts, however, did not show any considerable degree of segmental difference in number of neurones. Each abdominal segment of the crayfish carries a pair of appendages which are modified in different ways depending upon the segment: those of the first and second abdominal segments in the male are used as a genital organ, the third to fifth are swimmerets and the sixth is a uropod. A more precise count may therefore reveal segment-specific differences in neuron numbers representing segmental differences in the appendages.

Table 4. The number to efferent neurons, projecting interneurons and local interneurons

	Third abdominal	Terminal	
Total number of neurons	656	638[a] or	678[a]
Efferents	188 (29%)	233 (37%)	233 (34%)
Projecting interneurons	198 (30%)	136 (21%)	136 (20%)
Local interneurons	270 (41%)	269 (42%)	309 (46%)

[a] Two separate countings of different individuals

The five anterior abdominal ganglia show a common pattern of cell distribution, whereas the terminal ganglion differs significantly, probably resulting from ganglionic fusion (Kondoh and Hisada 1983). No matter how the terminal ganglion is constructed as a consequence of the fusion of the two ganglia, it has far fewer neurons than might be expected from a simple fusion of the two ganglia (Table 1). The distribution of the neuronal cell bodies (Fig. 1) also indicates that rather extensive modification has occurred in arrangement of cell bodies. An explanation of this could be that the fused posterior ganglion produces relatively few neurons because of a lack of appendages. Another factor to be considered is the possible elimination of unnecessary neurons by degeneration during neurogenesis, as is known to occur in insects (Goodman and Bate 1981; Truman and Schwartz 1983).

Central neurons constituting a ganglion in arthropods fall into three categories: efferent neurons, projecting interneurons and local interneurons. Their ratio to the total number of neurons has been estimated in the crayfish terminal ganglion (Reichert et al. 1982), the locust thoracic ganglia (Siegler and Burrows 1979) and the brain of the earthworm (Ogawa 1939). Our estimates with regard to the third abdominal and terminal ganglia of the crayfish are shown in Table 4. Their values nearly coincide with those obtained by Reichert (1982); either the third abdominal or the terminal ganglia contain about 20–30% of projecting interneurons, 30–40% of efferent neurons and 40–50% of local interneurons.

Serial homology and modification of neuropilar organization

Concentration of the nervous system by fusion of the segmental ganglia is omnipresent in insects and crustacea (Bullock and Horridge 1965). The present study reveals unambiguously that the terminal ganglion consists of two fused neuromeres, those of the intrinsic sixth abdominal ganglion and an 'seventh abdominal ganglion' (or 'telson ganglion'), as Monton (1928) suggested on embryological grounds. Each of them conforms to the same basic plan of commissure arrangement of that of the anterior five abdominal ganglia (Fig. 5). Many of the commissures are clearly homologous with those of A3 (Table 5). The most dorsal commissures, DCI-IV of A3, DCI-II of A6 and DCI of A7 are located above the DMT. The anterior intermediate commissures, VCI of A3 and A6, are characterized by thick neurites of intersegmental interneurons. The posterior intermediate commissures in all the abdominal ganglia, VCIII, contain the primary neurites of the LGs. The anteroventral commissures, the AVC of neuromeres A3, A6 and A7, which are located under VMT, contain primary neurites of intersegmental interneurons exclusively.

Table 5. The serial homology of the arrangement of commissures

Third abdominal	Terminal	
	A6 neuromere	A7 neuromere
DCI-II	A6DCI	A7DCI
DCIII-IV	A6DCII	
VCI	A6VCI	A7VCI-II
VCII-III	A6VCII-III	A7VCIII
AVC	A6AVC	A7AVC
PVC	–	A7PVC
–	–	A7SCI
HN	A6SCI	A7SCII

A prominent region of finely fibered neuropil, which lies across the midline at the ventroposterior part of the ganglion core, can be observed in all the abdominal neuromeres (HN in A3, SCI in A6 and SCII in A7). The most distinctive neuropilar areas within the terminal ganglion are A6SCI and A7SCI-II; these contain arborizations of primary afferents largely derived from mechanosensory hairs on the surface of the telson (Kondoh and Hisada in preparation). Similar structures are observed in many insect ganglia; they can be found, for example, in the thoracic ganglia of crickets (Wohlers and Huber 1985), in the cockroach (Gregory 1974) and in the locust (Tyrer and Gregory 1982), in which they designated as the *ventral association center* (VAC). The VAC in the locust is known to be projected by neurons from a variety of mechanosensitive sensory organs (Tyrer and Altman 1974; Tyrer et al. 1981; Pflüger et al. 1981).

Some considerable modification, reduction, compression and addition of commissures is evident, of a more extensive nature in the A7 neuromere than in other neuromeres. Firstly, PVC in A7 neuromere, accompanied by a finely fibered neuropil A7SCII, is more conspicuous than that of A3. No tract comparable to PVC in A3 could be found in neuromere A6. Secondly, the dorsal commissures (A6DCI-II and A7DCI) are so much reduced in number as well as being much smaller than in A3, that they can not be divided further into sub-tracts. Finally, an additional neuropil (A7SCI) lies across the midline at the anterior part of neuromere A7; this is a unique structure not found in any other anterior abdominal neuromeres. Such modifications of neuropil structure from a basic plan can also be observed in the fused ganglia of insects (Tyrer and Gregory 1982). It is still unknown, however, whether these modifications commonly observed in fused ganglia are attributable to the ganglionic fusion or not; they may simply represent a difference of segments.

The evidence that we present here shows that the plan exhibited by the fourth abdominal ganglion (Skinner 1985) is followed by all the other abdominal ganglia, including the fused, terminal ganglion, although little evidence is available that would enable us to generalize that this plan of crayfish abdominal ganglia can be found in all the other segments of crayfish, or, by extension, in other decapods.

Origin of the terminal ganglion and telson

In crustaceans, the segments are grouped into three tegmata according to the peculiarities of their shape or appendages.

These are the head, thorax and abdomen. One theory regarding the phylogenetic and embryonic constitution of segments (Borradaile et al. 1958) states that the body should be regarded as containing, besides the somites, an anterior presegmental region to which the eyes belong, and a postsegmental region (telson) in which the anus opens. Our evidence that the seventh abdominal neuromere exhibits a serial homology on topological organization of the neuropil appears to refute this theory. An alternative explanation is that the telson, although it lacks an appendage, may be the 'seventh abdominal segment' with the ganglion embryonically and serially homologous to the anterior ganglia.

If this is so, then, to which ganglion do the visceral cells (more than 70 cells associated with nerve R7 that innervates the hindgut at the caudal end of the crayfish terminal ganglion) belong? Winlow and Laverack (1972) supposed that it was the 'third fused ganglion', from which the visceral cells are derived. In each anterior abdominal ganglia there is an unpaired median neuron, the axon of which extends to nerve R7 at the anterior ventral margin of the cortex (Fig. 12C), thus giving some clues for consideration of the origin of the visceral cells and the seventh abdominal ganglion. It is likely that the embryonic origin of these cells and the visceral cells in the terminal ganglion are the same. Indeed, like the progeny of median neuroblast in the locust embryo (Goodman et al. 1980), these cells share a common physiological property of cell body excitability (J.J. Wine, personal communication). It is therefore reasonable to assume that visceral cells belong not to be 'hindgut ganglion' but to the 'telson (seventh abdominal) ganglion'. Their large number of their siblings may be attributed to the embryonic events in which their precursor cell(s) produce(s) far more progeny than the anterior counterparts, or that cell death diminishes the number of progeny in the six anterior ganglia (Goodman and Bate 1981; Truman and Schwartz 1983), although no evidence is available. Recent immunological investigation of the embryonic development of the terminal ganglion (J. Dumont and J.J. Wine, personal communication), however, supports our proposal that the terminal ganglion consists of two fused embryonic ganglia. It has been widely accepted that the hindgut in arthropods is formed by the invagination of the ectoderm in the last segment (the telson in a decapod) where the anus opens. It is therefore not so surprising that the 'telson ganglion' has many visceral neurons.

Acknowledgement. We are grateful to Drs. J. Dumont and J.J. Wine for their comments on the manuscript. We also thank Dr. Takahata and our colleagues for helpful discussions. This work was supported by a Grant-in-Aid (No. 56440006) from the Japanese Ministry of Education, Science and Culture to MH.

References

Abott NJ (1970) Absence of blood-brain barrier in a crustacean, *Carcinus maenas* (L). Nature 225:291–293

Abott NJ (1971) The organization of the cerebral ganglion in the shore crab, *Carcinus maenas*. I. Morphology. Z Mikrosk Anat Forsch 120:386–400

Allen EJ (1894) Studies on nervous system of crustacea. I. Some nerve elements of the embryonic lobster. Q J Microsc Sci 36:461–482

Altman JS, Bell EM (1976) A rapid method for the demonstration of nerve cell bodies in invertebrate central nervous systems. Brain Res 63:487–489

Bacon JP, Altman JS (1977) A silver intensification method for cobalt-filled neurones in wholemount preparations. Brain Res 138:359–363

Blest AD, Davie PS (1980) Reduced silver impregnations derived from the Holmes technique. In: Strausfeld NJ, Miller TA (eds) Neuroanatomical techniques insect nervous system. Springer, Berlin Heidelberg New York, pp 97–118

Borradaile LA, Potts FA, Eastham LES, Saunders JT (1958) The invertebrata (Third edition rev. by Kerkut GA). University Press, Cambridge

Bullock GE, Horridge GA (1965) Structure and function of the nervous systems of invertebrates. Vol. II, WH Freeman & Company, San Francisco

Chapple WD, Hearny ES (1976) The morphology of the fourth abdominal ganglion of the hermit crab: A light microscope study. J Morphol 144:407–420

Delcomyn F (1981) Nickel chloride for intracellular staining of neurons in insects. J Neurobiol 12:623–627

Goodman CS, Bate M (1981) Neuronal development in the grasshopper. Trens Neurosci 4:163–169

Goodman CS, Pearson KG, Spitzner NC (1980) Electrical excitability: A spectrum of properties in the progeny of a single embryonic neuroblast. Proc Natl Acad Sci USA 77:1676–1680

Gray P (1954) The neuroanatomist's formularly and guide. Constable, London

Gregory GE (1974) Neuroanatomy of the mesothoracic ganglion of the cockroach *Periplaneta americana* (L). I. The roots of the peripheral nerves. Philos Trans R Soc Lond [Biol] 267:421–465

Helm F (1928) Vergleichend anatomische Untersuchungen über das Gehirn insbesondere das 'Antennalganglion' der Dekapoden. Z Morphol Oekol Tiere 12:70–134

Hisada M, Takahata M, Nagayama T (1984) Structure and output connection of local non-spiking interneurons in crayfish. Zool Sci 1:41–49

Johnson GE (1924) Giant nerve fibers in crustaceans with special reference to *Cambarus* and *Palaemonetes*. J Comp Neurol 36:323–373

Kendig JJ (1967) Structure and function in the third abdominal ganglion of the crayfish *Procambarus clarkii* (Girard). J Exp Zool 164:1–20

Kondoh Y, Hisada M (1983) Intersegmental to intrasegmental conversion by ganglionic fusion in lateral giant interneurons of crayfish. J Exp Biol 107:515–519

Larimer JL, Kennedy D (1969) Innervation patterns of fast slow muscle in the uropods of crayfish. J Exp Biol 51:119–133

Macagno ER (1980) Number and distribution of neurons in leech segmental ganglia. J Comp Neurol 190:283–302

Maynard DM (1966) Integration in crustacean ganglia. Symp Soc Exp Biol 20:111–149

Mittenthal JE, Wine JJ (1978) Segmental homology and variation in flexor motoneurons of the crayfish abdomen. J Comp Neurol 177:311–334

Monton SM (1928) On the embryology of a mysid crustacean *Hemimysis lamornae*. Philos Trans R Soc [Biol] 212:363–463

Nagayama T, Takahata M, Hisada M (1983) Local spikeless interaction of motoneuron dendrites in the crayfish *Procambarus clarkii* Girard. J Comp Physiol 152:335–345

Ogawa F (1939) The nervous system of the eathworm (*Pheretima communissima*) in different ages. Sci Rep Tohoku Univ 13:395–488

Pantin CFA (1948) Notes on microscopical technique for zoologists. Cambridge, University Press

Pflüger HJ, Bräunig P, Hustert R (1981) Distribution and specific central projections of mechanoreceptors in locust thorax and proximal leg joints. II. The external mechanoreceptors: Hair plates and tactile hairs. Cell Tissue Res 216:79–96

Pitman RM, Tweedle DC, Cohen MJ (1972) Branching of central neurons: Intracellular cobalt injection for light and electron microscopy. Science 176:412–414

Quicke DLJ, Brace RC (1979) Differential staining of cobalt- and

nickel-filled neurones using rubeanic acid. J Microsc 115:161–163
Reichert H, Plummer MR, Hagiwara G, Roth RL, Wine JJ (1982) Local interneurons in the terminal abdominal ganglion of the crayfish. J Comp Physiol 149:145–162
Reichert H, Plummer MR, Wine JJ (1983) Identified nonspiking local interneurons mediate nonrecurrent, lateral inhibition of crayfish mechanosensory interneurons. J Comp Physiol 151:261–276
Retzius G (1892) Zur Kenntnis des Nervensystems der Crustaceen. In: Biologische Untersuchungen von Prof. Gustav Retzius. Central Druck, Stockholm, Sweden
Roth RL, Supper R (1973) Postembryonic addition of neurons to the abdominal nerve cord of the crayfish. Anat Rec 175:430
Sandeman DC, Luff SE (1973) The structural organization of glomerular neuropil in the olfactory and accessory lobes of an australian freshwater crayfish, *Cherax destructor*. Z Zellforsch Mikrosk Anat 142:37–61
Sandeman DC, Okajima A (1973) Statocyst induced eye movements in the crab *Scylla serrata*. III. The anatomical projections of sensory and motor neurons and the responses of the motor neurons. J Exp Biol 59:17–38
Selverston AL, Remler MP (1972) Neuronal geometry and activation of crayfish fast flexor motoneurons. J Neurophysiol 35:797–814
Siegler MVS, Burrows M (1979) The morphology of local nonspiking interneurones in the metathoracic ganglion of the locust. J Comp Neurol 183:121–148
Sigvardt KA, Hagiwara G, Wine JJ (1982) Mechanosensory integration in the crayfish abdominal nervous system: structure and physiological differences between interneurons with single and multiple spike initiating sites. J Comp Physiol 148:143–157
Skinner K (1979) The anatomical organization of crayfish segmental ganglia. Proc Soc Neurosci 5:262
Skinner K (1985) The structure of the fourth abdominal ganglion of the crayfish, *Procambarus clarki* (Girard). I. Tracts in the ganglionic core. J Comp Neurol 234:168–181
Stewart WW (1978) Functional connection between cells as revealed by dye-coupling with a highly fluorescent naphthalimide tracer. Cell 14:741–795
Strausfeld NJ (1976) Atlas of an insect brain. Springer, Berlin
Stretton AOW, Kravitz EA (1968) Neuronal geometry: determination with a technique of intercellular dye injection. Science 162:132–134
Takahata M, Nagayama T, Hisada M (1981) Physiological and morphological characterization of anaxonic non-spiking interneurons in the crayfish motor control system. Brain Res 226:309–314
Tyrer NM, Altman JS (1974) Motor and sensory flight neurones in a locust demonstrated using cobalt chloride. J Comp Neurol 157:117–138
Tyrer NM, Gregory GE (1982) A guide to the neuroanatomy of locust suboesophageal and thoracic ganglia. Philos Trans R Soc Lond [Biol] 297:91–123
Tyrer NM, Bacon JP, Davies CA (1979) Sensory projections from the wind-sensitive head hairs of the locust *Schistocerca gregaria*. Cell Tissue Res 203:79–92
Truman JW, Schwartz LM (1983) Programmed cell death in the nervous system of an adult insect. J Comp Neurol 216:445–452
Wiersma CA (1957) On the number of nerve cells in a crustacean central nervous system. Acta Physiol Pharm Neerl 61:135–142
Winlow W, Laverack MS (1972) The control of hindgut motility in the lobster *Homarus gammarus* (L). 3. Structure of the sixth abdominal ganglion and associated ablation and microelectrode studies. Mar Behav Physiol 1:93–121
Wohlers DW, Huber F (1985) Topological organization of the auditory pathways within the prothoracic ganglion of the cricket *Gryllus campeatris* L. Cell Tissue Res 239:555–565

Accepted September 26, 1985